University of Baghdad
College of Engineering
JOURNAL OF ENGINEERING

Journal of Engineering

journal homepage: www.jcoeng.edu.iq

Volume 31 Number 12 December 2025

Evaluation of the Performance of Self-Compacting Engineered Cementitious Composites (SCC-ECC) under Standard 28-day Water Curing

Mohammed Shaker Amouri *, **Nada Mahdi Fawzi**

Department of Civil Engineering, College of Engineering, university of Baghdad, Baghdad, Iraq

ABSTRACT

This study evaluates the performance of Self-Compacting Engineered Cementitious Composites (SCC-ECC) under standard 28-day water curing, aiming to develop a mixture with optimal flowability, high mechanical strength, and enhanced durability. Twenty-seven SCC-ECC mortar mixtures (without coarse aggregate) were prepared and tested according to EFNARC (2002) guidelines for self-compacting mortars. Fresh results (slump flow 240–260 mm, V-funnel 6–12 s, L-box >0.80) confirmed adequate flowability. In addition, direct tensile tests on dog-bone specimens demonstrated strain-hardening with multiple fine cracks and strain capacity exceeding 2%, verifying the ECC behavior. The mixtures were prepared with varying fly ash contents (20%, 25%, 30%), polyvinyl alcohol (PVA) fibers (1.5%–2.0%), and a high-range water-reducing admixture. The optimal mixture (R2) was identified based on superior results in compressive strength, flexural strength, impact resistance, water permeability, and elastic modulus. The selected mixture achieved compressive strength exceeding 70 MPa, flexural strength above 14 MPa, and impact energy absorption over 17,000 J, with very low chloride permeability (<750 Coulombs). Scanning Electron Microscopy (SEM) analysis confirmed a dense matrix and strong fiber–matrix bonding. The results demonstrate the feasibility of producing SCC-ECC with excellent fresh and hardened properties using industrial by-products and performance-enhancing additives, supporting the development of sustainable, high-performance composites for structural applications in aggressive environments.

Keywords: Self-compacting ECC, PVA fibers, Fly ash, Normal curing.

1. INTRODUCTION

Conventional concrete suffers from two major challenges: environmental impact due to high cement usage and mechanical limitations, particularly its low tensile ductility and susceptibility to cracking under tension **(Li, 2011)**. Ordinary Portland Cement (OPC) is the main binder in concrete and contributes significantly to CO_2 emissions. It is estimated that

*Corresponding author
Peer review under the responsibility of University of Baghdad.
https://doi.org/10.31026/j.eng.2025.12.07

Article received: 23/05/2025
Article revised: 21/09/2025
Article accepted: 30/09/2025
Article published: 01/12/2025

approximately one ton of CO_2 is released for every ton of cement produced, primarily due to the energy-intensive calcination process of limestone and the combustion of fossil fuels **(Abd Almajeed and Abbas, 2024)**.

In response to both environmental concerns and the mechanical performance limitations of conventional concrete, researchers have advanced the development of innovative cementitious materials, research has advanced toward the development of innovative cementitious materials. One such material is Engineered Cementitious Composites (ECC), commonly known as bendable concrete, which is distinguished by its exceptional tensile ductility—enabling strain capacities of up to 3–5%, far exceeding the typical 0.01% strain capacity of ordinary concrete **(Li, 2011; Salah et al., 2021)**. This remarkable ductility is achieved through the incorporation of micromechanically optimized polymer fibers, such as Polyvinyl Alcohol (PVA) or Polypropylene (PP), which facilitate the formation of multiple fine cracks instead of a single, catastrophic crack **(Li, 2012; Salah et al., 2021)**. In parallel, self-compacting concrete (SCC) has emerged as a revolutionary advancement to address placement difficulties in congested reinforcement zones. SCC flows under its own weight and fills complex formworks without mechanical vibration, ensuring uniformity and stability throughout the structure **(Salih and Ahmed, 2013)**.

Simultaneously, self-compacting concrete (SCC) has emerged as a solution to overcome workability issues in heavily congested reinforcement zones. SCC can flow under its own weight, filling complex formworks without the need for vibration, thereby reducing labor, noise, and construction time **(Yahia and Fawzi, 2017)**. Combining the advantages of ECC and SCC is the emergence of self-compacting engineered cementitious composites (SCC-ECC), which have excellent mechanical performance with workability. These features make SCC-ECC particularly well suited for elements of construction that require durability, mechanical strength and ease of use. Moreover, the environmental impact of concrete can be reduced by partial replacement of cement with eco-friendly materials such as limestone powder, silica fume, fly ash, and ground granulated blast furnace slag (GGBFS) **(Qais and Abbas, 2024; Yahia and Fawzi, 2017)**. These materials not only enhance the performance characteristics of concrete but also contribute to reducing CO_2 emissions and promoting circular economy principles through the recycling of industrial by-products **(Sara et al., 2021; Li, 2012).** The ordinary Portland cement significantly reduced in polyvinyl alcohol fiber-reinforced ECC, by high percentage substitution with a fly ash–sugarcane bagasse ash blend, performed with 25.58 MPa of compressive strength after 28 days, which is greater than 20.7 MPa **(ASTM C270-19, 2019)** despite being lower than those that used either higher cement amount or slag mixes. This result indicates the possibility of making environmentally friendly ECC with reasonable strength based on the combined use of recycled materials **(Yaseen et al., 2023)**

The contribution of microcracking to the ECC and its effect on water absorbance have been emphasized by **(Şahmaran and Li, 2009).** It was discovered that, although microcracks were induced by mechanical loading, ECC still exhibited better resistance to water transport than normal concrete, especially when water-repellent admixtures were applied. This is an outcome of ECC's controlled width of crack and its ductile nature. **(Pontes et al., 2021)** evaluated four types of test methods to determine the chloride penetration resistance of concrete and found that fly ash helped to refine the structure of the pores of cement paste, resulting in a reduction of chloride penetration. It also clarified that the sensitivity of the test was changeable according to fly ash content, which emphasized the necessity of correct choices of durability assessment methods. **(Li, 2012)** presented ECC as a novel material,

whose basic characteristic was to change the brittle nature of the conventional concrete in a ductile, damage-tolerant composite, with strain capacities of 3–5%, a higher value than ordinary concrete. This characteristic enables the ECC to inhibit crack opening under tensile loading, resulting in much better durability and mechanical performance.

However, conventional concrete still suffers from major drawbacks such as limited tensile ductility, poor crack resistance, and significant environmental impact due to high cement consumption. These shortcomings highlight the research gap for the development of advanced cementitious composites that combine superior mechanical performance with improved sustainability. In this context, self-compacting engineered cementitious composites (SCC-ECC) were chosen because they provide both excellent workability in congested reinforcement areas and enhanced ductility and durability through fiber reinforcement.

The purpose of this study is to evaluate the performance of SCC-ECC mixtures under normal 28-day curing, with the aim of optimizing their mechanical properties (compressive strength, flexural strength, impact resistance, and elastic modulus) as well as durability characteristics (water permeability and chloride resistance). By addressing this gap, the research demonstrates the feasibility of producing sustainable, high-performance concrete suitable for aggressive environments.

2. EXPERIMENTAL WORK

2.1 Materials

2.1.1 Cement

The ordinary cement has been used in this research, class 42.5R, which complies with the (**Iraqi Standard No. 5, 2019)**. Its physical and chemical properties are detailed in **Table 1.**

Table 1. Chemical and physical properties of ordinary Portland cement.

Oxides	OPC	Specification according to (Iraqi standard No.5, 2019)
SiO_2	18,68	-
Al_2O_3	7.70	-
Fe_2O_3	1,95	-
CaO	63.01	-
MgO	4.32	≥5.0%
SO_3	2.32	≥2.8%
L.O.I	0.95	≥4.0%
Specific gravity	3.15	-
Blaine fineness, cm^2/gm	4324	≤3000

2.1.2 Fly Ash

The fly ash Type F utilized in this study is characterized as a fine, glass-like powder produced through the combustion of coal. The chemical composition of it is detailed in **Table 2.** As per this investigation, the fly ash utilized in the study complied with **(ASTM C618, 2023).**

Table 2. Chemical composition of fly ash

Oxide	Contents, %	(ASTM C618, 2023) Requirement
Fe_2O_3	5.33	The sum of values more than 50%
Al_2O_3	17.57	
SiO_2	65.52	
SO_3	0.83	Max. 5%
MgO	0.83	--
CaO	0.96	--
L.O. I	2.79	Max. 6%
K_2O	2.35	--
Na_2O	1.34	--

2.1.3 Water

The Tap water used in the mixture is compliant with **(Iraqi Standard IQS. 1703, 2018)**.

2.1.4 Fine Aggregate

The fine aggregate used in this study was sourced from northern Iraq. Classified as Zone Two, it adhered to the physical and chemical property requirements outlined in the (**Iraqi Standard IQS No. 45,1984)**. Detailed properties of the sand are presented in **Tables 3** and **4.**

Table 3. Sieve analysis (gradation) of fine aggregates

Size of the Sieve,mm	Cumulative percentage pass	(Iraqi Standard IQS. 45, 1984), zone2
10	100	100
4.750	93	90-100
2.360	85	75-100
1.180	76	55-90
0.60	54	35-59
0.30	24	8-30
0.150	8	0-10

Table 4. Physical and chemical properties of sand.

Physical characteristics	Tests results	(Iraqi Standard IQS. 45, 1984)
Density (kg/m³)	1592	----
Fineness modulus	2.72	----
Specific gravity	2.62	----
Absorption, percent	1.2	----
Fine materials that pass through 75 µm sieve	1.4	3% maximum
Sulfate content, percent	0.15	0.5% maximum

2.1.5 PVA Fibers

Polyvinyl alcohol (PVA) fibers are synthetic polymer fibers widely used in engineered cementitious composites due to their high tensile strength, good alkali resistance, and ability to control crack widths through fiber bridging. The main physical properties of the fibers are summarized in **Table 5**, while their appearance is shown in **Fig. 1.**

Table 5. Polyvinyl alcohol fiber (PVA) properties- according to the manufacturer * data sheet (Shandong Jinhongyao Engineering Material Co. Ltd, China).

Item	Content	Unit	Standard
1	**Melting point**	°C	217
2	**Tensile strength**	MPa	1789
3	**Modulus of Elasticity**	GPa	57
4	**Ultimate elongation**	%	<30
5	**Length**	mm	(8-11)
6	**Diameter equivalent**	µm	42
7	**Alkali resistance**	%	≥95
8	**Safety**		Non-toxic
9	**Elongation at break**	%	7
10	**Hot water resistance**	°C	≥98
11	**Density**	g/cm^3	1.28

* According to the Manufacturer

Figure 1. Polyvinyl alcohol fiber

2.1.6 Superplasticizer

Sika® Visco Crete®-180 GS is a high-performance admixture designed for concrete and mortar. It functions as a set retarder, a high-range water reducer, and a superplasticizer, utilizing Sika's advanced third-generation polycarboxylate polymer technology, known as 'Visco Crete® '. The ECC workability was improved to **(ASTM C494, 2013)**. The properties of superplasticizer are shown in **Table 6.**

Table 6. Properties of the superplasticizer (Sika® ViscoCrete®-180 GS, Sika AG – Switzerland; distributed by Sika Iraq)* .

Properties	Descriptions
Color	Black / Dark brown liquid
Air entrainment	< 1.0%
Calcium Chloride content	Nil
Specific gravity	1.22 – 1.24 at 20°C
Chloride content	Nil

* According to the manufacturer

2.2 Experimental Program

For the three kinds of ECC concrete, twenty-seven different mixtures using fibers, cementitious materials, and superplasticizer were tested to assess their impact on segregation resistance and filling ability.

All mixtures in this study used a cementitious material content of 845 kg/m^3, 270 kg/m^3 of water, and 570 kg/m^3 of sand. For the first time, the study examined the effects of different fly ash replacement levels (30%, 25%, and 20%) on compressive strength at both 7 and 28 days, as detailed in **Table 7**. These mixtures were selected based on their ability to meet flow requirements specified by **(EFNARC, 2002)**. It should be emphasized that the mixes are mortar-type ECC without coarse aggregate. Therefore, the evaluation of fresh properties followed **(EFNARC, 2002)** guidelines for self-compacting mortars, which specify slump flow of 240–260 mm and V-funnel time of 6–12 s, rather than the ranges for full SCC concrete. This methodology is consistent with the approach of **(Raharjo et al., 2013)**, who evaluated various SCC compositions using fly ash, silica fume, and iron slag to achieve optimal flow and compressive strength performance.

Additionally, one mixture from each group (R2, R11, and R20) was selected for flexural strength testing at 28 days. These mixtures had identical fiber and superplasticizer contents but varied in cement and fly ash proportions. The results showed that mixture R2 demonstrated the highest flexural performance and the greatest compressive strength at 28 days of curing, as shown in **Table 8**. Therefore, R2 was selected as the reference mixture for this study due to its superior mechanical and workability performance, consistent with the optimization strategies reported by **(Qorllari and Bier, 2022)**.

Table 7. Trail mix of ECC concrete

Mix No.	Cement kg/m^3	Fly Ash (%)	Fly Ash kg/m^3	SP (%)	Fiber (%)*	Slump Flow (mm)	V-Funnel Time (s)	Compressive Strength at 7 days	Compressive Strength at 28 days	Flexural Strength (MPa) At 28 days
R1	650	30	195	1.5	1.5	240–260	10–12	49.5	64.2	12.7
R2	650	30	195	1.75	1.5	260–280	9–11	54.4	71.3	14.1
R3	650	30	195	2.0	1.5	280–300	8–10			
R4	650	30	195	1.5	1.75	220–240	11–13			
R5	650	30	195	1.5	2.0	200–220	12–14			
R6	650	30	195	1.75	1.75	240–260	10–12	47.2	62.3	12.3
R7	650	30	195	2.0	1.75	260–280	9–11	39.6	52.5	10.4
R8	650	30	195	1.75	2.0	220–240	11–13			
R9	650	30	195	2.0	2.0	240–260	10–12	46.4	61.1	12.1
R10	715	20	130	1.5	1.5	220–240	11–13			

R11	715	20	130	1.75	1.5	240–260	10–12	52.8	69.3	13.7
R12	715	20	130	2.0	1.5	260–280	9–11	58.4	78.4	15.5
R13	715	20	130	1.5	1.75	200–220	12–14			
R14	715	20	130	1.75	1.75	220–240	11–13			
R15	715	20	130	2.0	1.75	240–260	10–12	59.1	79.3	15.7
R16	715	20	130	1.5	2.0	180–200	13–15			
R17	715	20	130	1.75	2.0	200–220	12–14			
R18	715	20	130	2.0	2.0	220–240	11–13			
R19	633.75	25	211.25	1.5	1.5	230–250	10–12	46.2	60.3	11.9
R20	633.75	25	211.25	1.75	1.5	250–270	9–11	53.92	70.4	13.9
R21	633.75	25	211.25	2	1.5	270–290	8–10	43.3	58.7	11.6
R22	633.75	25	211.25	1.5	1.75	210–230	11–13			
R23	633.75	25	211.25	1.75	1.75	230–250	10–12	47.1	62.2	12.3
R24	633.75	25	211.25	2	1.75	250–270	9–11	46.4	61.4	12.1
R25	633.75	25	211.25	1.5	2	190–210	12–14			
R26	633.75	25	211.25	1.75	2	210–230	11–13			
R27	633.75	25	211.25	2	2	230–250	10–12	51.3	68.5	13.6

Table 8. The results of compressive, flexural strength and L-Box

Mix Number	Compressive Strength (MPa) At 28 days	Flexural Strength (MPa) At 28 days	Comp./Flex. ratio	L-Box Ratio (H2/H1)
R2	71.3	14.1	19.77%	0.92
R20	70.4	13.9	19.74%	0.89
R11	69.3	13.7	19.76%	0.85

The L-box test was conducted in accordance with EFNARC (2002) guidelines for self-compacting mortars, considering the mortar-like behavior of ECC due to the absence of coarse aggregates. As shown in **Fig. 2**, all selected mixtures achieved blocking ratios above 0.80, confirming their self-compacting capability.

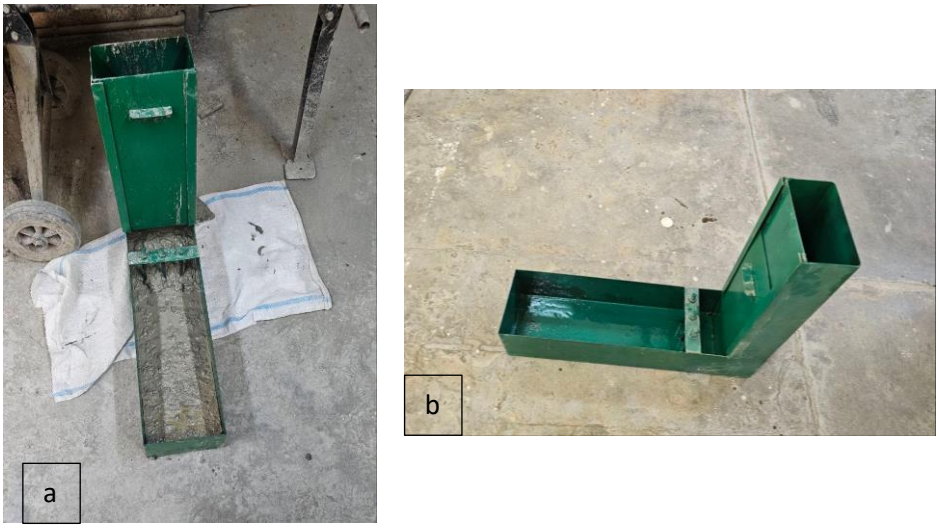

Figure 2. Experimental setup of the L-box test apparatus. (a) after testing and (b) before testing

To further verify the tensile strain-hardening behavior of the SCC-ECC mixtures, direct uniaxial tension tests were performed on dog-bone-shaped specimens prepared from the three shortlisted mixtures (R2, R20, and R11) as shown in **Figs. 3 and 4**. This test method follows the procedures commonly adopted for ECC characterization, as described by (**Li, 2007)**, since there is no dedicated ASTM standard for direct tensile testing of fiber-reinforced cementitious composites. Three specimens were cast and water-cured for 28 days under normal curing conditions for each mixture. The tests were conducted using a servo-hydraulic universal testing machine under displacement control at a loading rate of 0.2 mm/min, and the tensile stress–strain response was recorded continuously until specimen failure.

Figure 3. Dog-bone specimens of SCC-ECC mixtures (R2, R20, and R11) prepared for direct tensile strain-hardening test.

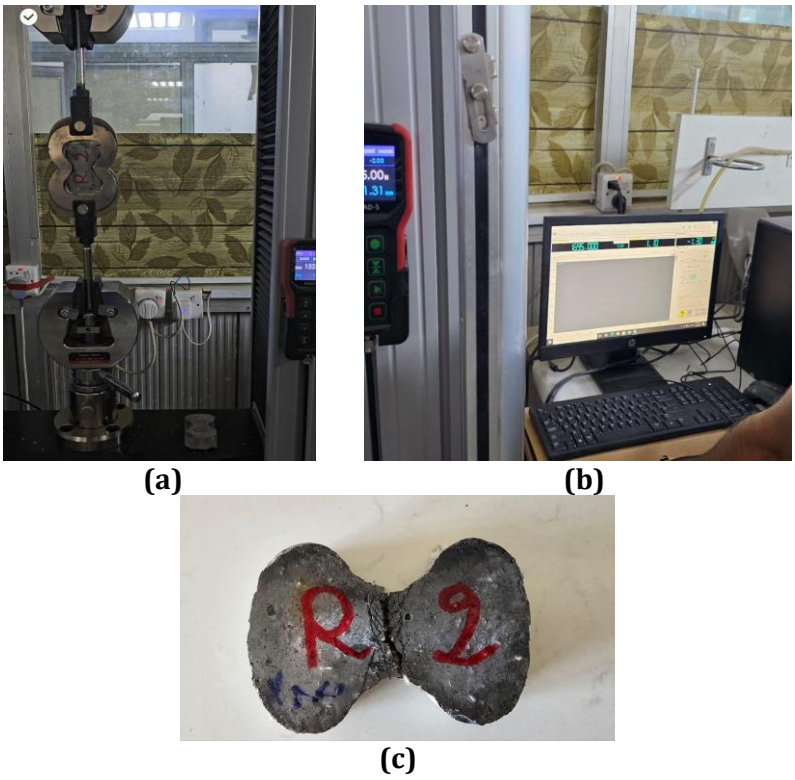

Figure 4. Dog-bone specimens of SCC-ECC mixtures under direct tensile test: (a) specimen mounted in the testing machine during loading, (b) monitoring of stress–strain data acquisition, and (c) specimen after failure showing the final dominant crack and residual fine cracks within the gauge length.

The following parameters were determined:

- First-cracking tensile strength (σcr)
- Ultimate tensile strength (σu)
- Strain capacity (εu)
- Ratio σu/σcr
- Multiple cracking behavior (number of cracks within the gauge length)
- Average crack width at peak load

Table 9. Direct tensile test results of SCC-ECC mixtures (R2, R20, R11) at 28 days

Mix Number	σcr (MPa)	σu (MPa)	σu/σcr	εu (%)	Avg. crack width (μm)	No. of cracks
R2	2.8 – 3.4	3.8 – 4.8	1.25 – 1.45	2.0 – 2.5	50 – 100	10 – 18
R20	2.6 – 3.2	3.5 – 4.5	1.25 – 1.40	1.6 – 2.2	60 – 120	8 – 15
R11	2.4 – 3.0	3.2 – 4.2	1.20 – 1.35	1.4 – 2.0	70 – 130	7 – 13

The results are summarized in **Table 9**, which clearly demonstrates that all three mixtures exhibited strain-hardening behavior (σu > σcr and εu ≥ 1.4%), with mixture R2 outperforming the others in terms of strain capacity, crack distribution, and controlled crack widths (<100 mico). The average crack widths were determined using optical microscopy and high-resolution image analysis during the direct tensile test, following the procedures

reported by **(Li, 2007; Zhang et al., 2019).** This approach is sufficient to measure crack openings within the range of 50–150 mico.

2.3 Testing

2.3.1 Compressive Strength

The specimen with dimensions (75*150mm) tested compressive strength according to **(ASTM C39-21, 2021)** used for this test with as shown in **Fig. 5.**

Figure 5. ECC compressive strength test

2.3.2 Flexural Strength

The test was carried out according to **(ASTM C 348-21, 2021)** to test the one-point load flexural strength of the ECC Prisms from the selected mixture R2 as shown in **Fig. 6**. The flexural strength of each combination was determined by testing an average of three prism specimens (40mm x 40mm x 160mm) after curing at ages 28 days to determine flexural strength, the following equation was used:

$$S_f = 0.0028\ P \quad (1)$$

Where:
S_f : the flexural strength (MPa)
P Maximum load is denoted by (N)

Figure 6. ECC Flexural Test

2.3.3 Impact Resistance Test

These tests were carried out according to **(ACI C544.2R, 2009)**. Three cylinders with dimensions of (150*63.5mm) were tested at 28 days of curing time, as shown in **Fig. 7.** The impact energy absorption was calculated according to **(ACI 544.2R,2009)** using:

$$Energy(j) = N * W * H \quad (2)$$

where N is the number of blows, W is the hammer weight (44.5 N), and H is the drop height (0.457 m). The energy per blow was calculated as 20.33 J.

Figure 7. ECC specimen under impact load – before and after failure

2.3.4 Water Permeability Test

This test was made according to **(EN 12390-8, 2019)**, where three cubes of (150×150×150) mm after 28 days of curing ages as a reference where the tests take 72 hr. while the water was pressured with 5bar a hydraulic device after that measuring the depth of water in sample as shown in **Fig. 8** The results was evaluated according to **(DIN 1048-5,1991).**

Figure 8. Water Permeability Test of ECC Samples

2.3.5 Static Modulus of Elasticity Test

The static modulus of elasticity test conducted in accordance with **(ASTM C469, 2022)** is a crucial assessment for evaluating the stiffness and deformation characteristics of concrete under uniaxial compressive stress. The static modulus of elasticity (E) provides valuable insights into the material's resistance to deformation, which is essential for structural design

and performance evaluation. This experiment was performed on three standard cylindrical concrete specimens of 150 × 300 mm at an age of 28 days, as shown in **Fig. 9**

Figure 9. Static modulus of elasticity test of ECC samples

Calculation of Elastic Modulus: The static modulus of elasticity (E) was computed using the equation:

$$E = (S_1 - S_2) \div (\varepsilon_2 - 0.000050) \quad (3)$$

where:
E = Static modulus of elasticity (MPa)
S_2= Stress at 40% of ultimate load (MPa)
S_1= Initial stress
ε_2 = Corresponding strain at 40% of ultimate load
The Poisson's ratio (μ) was determined as:

$$\mu = (\varepsilon_{t2} - \varepsilon_{t1}) \div (\varepsilon_2 - 0.000050) \quad (4)$$

Where:
ε_{t2} = Transverse strain at mid height of the specimen produced by stress S_2.
ε_{t1} = Transverse strain at mid height of the specimen produced by stress S_1.
ε_2 = Corresponding strain at 40% of ultimate load.
The measured results were compared with theoretical values obtained from (**ACI 318-19, 2019; EN 1992-1-1, 2004)**, as shown in **Table 9.**

Table 10. Comparison of computed static modulus of elasticity with design codes

Calculation	Compressive Cylinder Strength $f\acute{c}$ (MPa)	Static Modulus of Elasticity (MPa)
Actual Test Results (ASTM C469-22, 2022)	measured value	measured value
Theoretical Equation (ACI 318-19, 2019)	(measuring value)	$Ec = 4700\sqrt{f\acute{c}}$
EN 1992-1-1, 2004 (Theoretical Equation)	$fcm = f\acute{c} + 8$	$Ecm = 22 \times (\frac{fcm}{10})^{0.3}$

2.3.6 Chloride Penetration Test

The Chloride Penetration Test, also known as the rapid chloride permeability test (RCPT), is conducted according to **(ASTM C1202, 2022)** This test evaluates the concrete's ability to resist chloride ingress, which is a critical factor in assessing durability, especially for structures exposed to marine environments or deicing salts. The permeability of the concrete is classified based on the total charge passed (Coulombs) during the test as shown in **Table 11.**

Table 11. Chloride permeability classification based on total charge passed

Total Charge Passed (Coulombs)	Chloride Permeability Classification
> 4000	High
2000-4000	Moderate
2000-1000	Low
100-1000	Very Low
< 100	Negligible Permeability

3. RESULTS AND DISCUSSION

3.1 Compressive Strength

In this study, three concrete cylinders were tested after 28 days of water curing to evaluate the compressive strength of the produced ECC. The results, summarized in **Table 12**, reflect the material's ability to meet the acceptable strength requirements. The compressive strength test was conducted in accordance with **(ASTM C39-21,2021)**. The results obtained are consistent with those reported by **(Ghafor et al., 2022),** who highlighted the importance of standard cylinder testing in assessing ECC performance.

The results of the present investigation are in good agreement with the results reported in the literature by **(Lepech and Li, 2008)** for ECC fabricated under well-defined mixing and curing conditions, where compressive strengths of more than 60 MPa were obtained, thus confirming the applicability of this kind of ECC for a variety of engineering applications.

The attained strengths are in accordance with those reported by **(Li and Kanda, 1998)**, who noted that ECC can achieve compressive strength from 30 to 70 MPa, depending on mix proportions and curing regimes, with excellent ductility and microcracking controlling properties. Moreover, that phenomenon verifies with the findings of **(Li, 2007)** that ECC not only possesses highly competitive compressive strength when compared to (high-strength concrete), but to a great extent, it can also be durable and cracking-resistant so as to ensure a durable behavior of the structure in service.

Table 12. Compressive strength test result for SCC-ECC

Mix	Comp. Strength at 28 days (Mpa)	Variation
R2-1	70.4	%1.21
R2-2	71.5	
R2-3	72.1	

3.2 Flexural Strength

The flexural strength test results are shown in **Table 13.** The experimental procedure is similar to that reported by **(Krishnaraja and Kandasamy, 2018)** in which the flexural behavior of hybrid ECC-layered reinforced concrete beams was investigated with identical specimen dimensions and curing conditions. The high flexural strength of this work supports the observations of **(Choucha et al., 2018)** found strong correlation between compressive and flexural strengths in ECCs containing natural pozzolans, thereby verifying that a reliable means for testing flexural strength is similarly an indication for overall strength. Moreover, the selection of specimen size and testing setup adopted in this work is in agreement with the indications provided in **(Nalon et al., 2018)** who highlighted the effect of specimen geometry on the accurate evaluation of mechanical properties when specifically testing cementitious materials with superior ductility like ECC. Also, the results from the results from the developed ECC mixtures have high flexural performance than the conventional mixes, are in agreement with the results of **(Insabi and Sankaranarayanan, 2020)** as ECC mixes showed a higher tensile and flexural strength than standard M25 concrete, making them suitable for structural applications that call for crack resistance and energy absorption.

Table 13. Flexural strength test result for SCC-ECC

Mix	Flexural Strength at 28 days (Mpa)
R2-1	13.8
R2-2	14.2
R2-3	14.5

3.3 Impact Resistance Test

The impact resistance test conducted after 28 days of curing, as detailed in **Table 14** and **Fig. 10**, demonstrates that the SCC-ECC specimens exhibit significantly enhanced impact resistance. This improvement is primarily attributed to the interlocking fiber network within the matrix, which effectively dissipates impact energy and restricts crack propagation, leading to increased energy absorption capacity. Similar findings were reported by (**Al-Ameri et al., 2022)**, who demonstrated that ECC reinforced with synthetic fibers exhibits superior impact resistance due to the energy dissipation mechanisms provided by the fiber bridging effect.

Based on this, the total energy absorption at the first crack and failure stages for each mix is summarized in **Table 13**. This calculation approach is consistent with the methodology described by **(Santhi et al., 2014)**, who utilized the same equation in their investigation of fiber-reinforced concrete impact performance, confirming its validity for quantifying energy absorption under repeated impact loads. Findings show that mix R2-3 emulated the maximum energy absorption of all the mixes examined. This finding is consistent with the study of **(Abid et al., 2022)**, fibrous concrete shows high resistance to failure impact as the dosage of fiber increases and the design of the mixture becomes optimized, resulting in a resilient response against repeated impact loads.

Also, the consideration of the results for the indication of structural improvement in performance is encouraged by **(Murali et al., 2014),** who proved that fiber addition in concrete increases energy absorption and safety under provisions of drop-weight impact (important for structures affected by dynamic or accidental load).

Table 14. Impact and energy absorption test result for SCC-ECC

Mix	First Crack (No.)	Failure (No.)	First Crack (J)	Failure (J)
R2-1	755	830	15,353	16,875
R2-2	762	841	15,498	17,114
R2-3	769	853	15,643	17,351

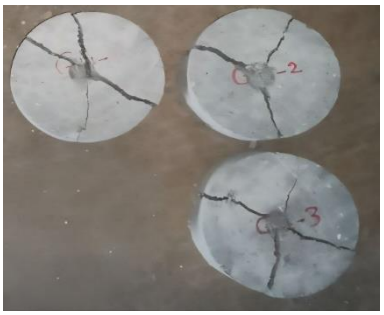

Figure 10. Impact test of SCC_ECC samples after failure

3.4 Water Permeability

The water permeability of ECC mixtures was evaluated according to **(EN 12390-8, 2019)** and **(DIN 1048-5, 1991),** by measuring the depth of water penetration under hydraulic pressure. This method provides a reliable criterion to assess concrete durability, as lower penetration depths indicate higher resistance to moisture ingress. The results obtained in this study confirmed the superior impermeability of ECC, which is consistent with findings reported in previous studies **(Lepech and Li, 2009; Naderi et al., 2018).**

The results of the water permeability test **Table 15** indicate that the penetration depth of the R2 mixture specimens ranged between 0.42 and 0.53 mm, which corresponds to low to very low permeability ratings. Such consistently low values confirm the dense microstructure of SCC-ECC, where fiber bridging and the refinement of microcracks effectively block continuous pathways for water ingress. The small variations among specimens reflect the uniformity of the mix design and the effectiveness of the curing regime. These findings are in agreement with **(Skutnik et al. 2020)** and are further supported by **(Safarkhani and Naderi 2023)**, who highlighted that fiber reinforcement and microstructural densification play a crucial role in reducing water penetration in cementitious composites. In addition to the water permeability test, SEM scanning electron microscopy was used to test the microstructure, as shown in **Fig. 11.**

Table 15. Water permeability test result for SCC-ECC.

Mix	Water Penetration Depth (mm)	Permeability Rating
R2-1	0.53	Low
R2-2	0.47	Low
R2-3	0.42	Very Low

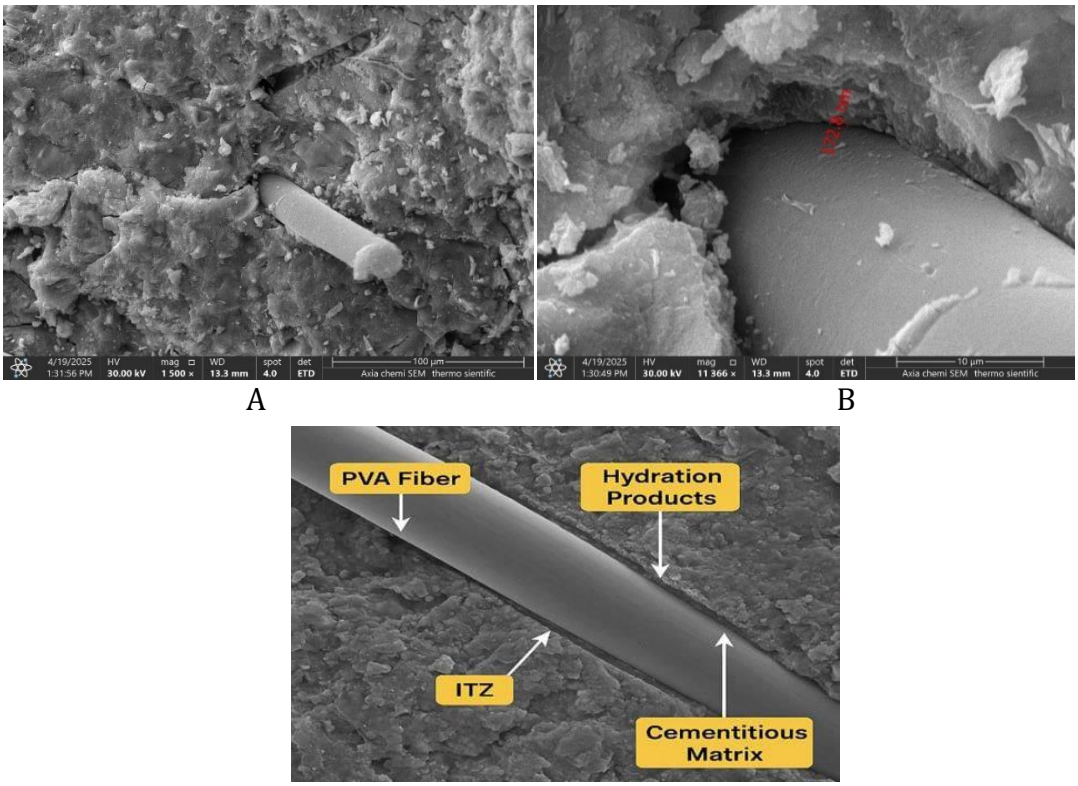

A B

C

Figure 11. SEM test of SCC-ECC Sample A: Sem with 100mico, B Sem in 10mico, C description of containing picture.

The SEM observation revealed highly dense micro-structure and weak pore connection of the ECC matrix; to obtain a ground of explanation of the low water permeability of the performance of the experimental results. The Overall judgment from the integrated evaluation indicates that ECC is suitable for manufacturing applications with high resistance to moisture and hydraulic pressure.

These images clearly show the interaction of the Polyvinyl Alcohol (PVA) fibers with the average cementitious matrix, as well as the ITZ. The ITZ is a key controlling zone for stress transferring, crack propagation arrest and the global mechanical performance of ECC. From these images, ITZ seems well-developed and free of visible voids or microcracks. The interface between fiber and matrix reveals no debonding or pullout, and well-bonding of matrix and fiber can also be verified. This observation was agreed with those of **(Wang et al., 2023)** that a denser fiber–matrix interface and reduced difference between ITZ and matrix improves the performance of composite.

In addition, the fiber surfaces are still homogeneously covered with hydration products, indicating continuing pozzolanic reactions and matrix densification in the vicinity of the interface. This was consistent with the findings of **(Shen et al., 2022)** who showed that PVA fibers accelerate hydration product growth at the interface, resulting in more densification of the matrix when fly ash is used. The absence of porous or loosely packed regions surrounding the fibers further supports the conclusion that the ITZ in this ECC mixture is compact and structurally sound. This observation is supported by Peng (**Zhang et al., 2019)**,

who concluded that PVA fibers contribute to refining the pore structure and enhancing the microstructural integrity of cementitious composites.
Such a high-quality ITZ is essential for enabling the unique strain-hardening and crack-bridging behavior of ECC. The integrity of the fiber-matrix interface ensures effective stress transfer and limits crack widths, which are fundamental for achieving superior durability and ductility. This behavior is further confirmed by **(Zhang et al., 2023)**, who demonstrated that improved chemical bonding and frictional properties at the fiber-matrix interface are key to achieving superior mechanical performance in fiber-reinforced composites. Finally, the performance of ECC under aggressive environmental conditions, including wet–heat–salt coupling environments, which will be examine tested in the next step, benefits significantly from the presence of PVA fibers, as they enhance the resistance to permeability and chloride penetration. This is in agreement with the findings of **(Zhang et al., 2023)**, who showed that ECC with optimized PVA fiber content achieves enhanced durability under severe exposure conditions.

3.5 Static Modulus of Elasticity Results

The results of a static modulus of elasticity and Poisson's ratio test for an ECC concrete specimen as shown in **Tables 16** and **17.**
The experimental results obtained for the two tested specimens, R2-1 and R2-2, demonstrate promising mechanical performance in terms of both compressive strength and elastic modulus. The measured compressive strengths of 61.54 MPa for R2-1 and 62.53 MPa for R2-2 indicate that the designed ECC mixtures achieved high strength levels, which are generally considered favorable for structural applications requiring both durability and load-bearing capacity. This aligns with the findings of **(Xiong et al., 2021)**, who confirmed that ECC incorporating ceramic waste under optimal curing conditions can achieve comparable or even higher compressive strengths suitable for structural use.

Table 16. Static modulus of elasticity test results for SCC-ECC.

Mix	Input Data		Calculated Results	
R2-1	Dial Gauge Reading (Longitudinal)	27 divisions	Stress at 40% Load	24.62 MPa
	Dial Gauge Reading (Lateral)	4 divisions	Longitudinal Strain	0.00135
	Gauge Sensitivity	0.01 mm/div	Static Modulus of Elasticity(E)	18234 MPa
	Gauge Length (Longitudinal)	200 mm	Poisson's Ratio (μ)	0.198
	Specimen Diameter	150 mm		
	Load at 40% Ultimate	435 kN		
R2-2	Dial Gauge Reading (Longitudinal)	25 divisions	Stress at 40% Load	25.01 MPa
	Dial Gauge Reading (Lateral)	5 divisions	Longitudinal Strain	0.00125
	Gauge Sensitivity	0.01 mm/div	Static Modulus of Elasticity(E)	20010 MPa
	Gauge Length (Longitudinal)	200 mm	Poisson's Ratio (μ)	0.267
	Specimen Diameter	150 mm		
	Load at 40% Ultimate	442 kN		

Table 17. Comparison of static modulus of elasticity calculations

Calculation	Compressive Cylinder Strength f'c (MPa) R2-1	Static Modulus of Elasticity (MPa) R2-1	Compressive Cylinder Strength f'c (MPa) R2-2	Static Modulus of Elasticity (MPa) R2-2
Actual Test Results (ASTM C469)	61.54	18234.0	62.53	20010.0
ACI 318 (Theoretical Equation)	61.54	36870.0	62.53	37166.0
Eurocode 2 (Theoretical Equation)	61.54	39363.0	62.53	39531.0

When comparing the experimentally determined static modulus of elasticity values with those predicted by theoretical equations from **(ACI 318-19, 2019; EN 1992-1-1, 2004)**, it is evident that the actual values (18,234 MPa for R2-1 and 20,010 MPa for R2-2) are lower than the theoretical estimates (approximately 37,000–39,500 MPa). This deviation is consistent with the mechanical behavior of ECC materials, as reported by **(Ding et al., 2020)**, who showed that ECC typically exhibits lower Static Modulus of Elasticity compared to conventional concrete due to its fiber-reinforced, aggregate-free matrix structure that favors ductility over stiffness. Despite this deviation, the experimental results are considered satisfactory and align well with the expected performance of ECC materials. Similar observations were reported by **(Choucha et al., 2018)**, who found that ECC mixtures with natural pozzolana displayed predictable relationships between compressive strength and elastic modulus, supporting the reliability of using strength as a primary indicator of overall performance.

The consistency between the two tested specimens further supports the reliability of the mixtures and the experimental procedure. This conclusion is supported by the work of **(Li, 2007)**, who emphasized the importance of achieving a balance between strength, ductility, and crack control in ECC to ensure its structural efficiency and durability, even if this comes at the expense of lower stiffness compared to conventional concrete.

3.6 Chloride Penetration Test

This test evaluates the total electrical charge passed through concrete specimens under a constant voltage over a six-hour period, providing an indirect measure of chloride penetrability. This testing approach aligns with the findings of **(de Jesus et al., 2025)**, who demonstrated that **(ASTM C1202, 2022)** effectively differentiates between concretes with varying cement types and their chloride resistance performance.

In the present study, ECC specimens with a fly ash-to-cement ratio (FA/PC = 0.3) were evaluated for chloride ion permeability after 56 days of continuous immersion in potable water. This curing condition aims to simulate the exposure of structural elements in non-aggressive environments. Similar curing strategies were adopted by **(Wu et al., 2021)**, who evaluated the chloride resistance of ECC-based soil nail systems and confirmed the benefits of fiber reinforcement and controlled microcracking in limiting chloride ingress. The results summarized in **Table 18** and **Fig. 12**, indicate that the specimens exhibited very low chloride ion penetrability, with measured charges ranging between 663 and 750 Coulombs.

According to **(ASTM C1202, 2022)** classification, these values fall within the "Very Low" category, reflecting the excellent resistance of the ECC matrix to chloride ingress under normal water curing conditions. These findings are consistent with the work of **(Turk et al., 2022)**, who reported that ECC mixtures incorporating high-volume fly ash and limestone powder demonstrated superior resistance to chloride penetration, attributed to matrix densification and refined pore structure.

Table 18. Comparison of static modulus of elasticity calculations

Mix	RCPT (Coulombs)	Chloride Permeability Classification
R2-1	750	Very Low
R2-2	723	Very Low
R2-3	663	Very Low

Figure 12. Chloride penetration test of SCC-ECC sample

Moreover, the interpretation of RCPT results as a reliable indicator of concrete durability has been supported by **(Shi, 2004)**, who highlighted that although RCPT primarily measures electrical conductivity, it remains a practical and widely adopted method for evaluating chloride penetrability in concrete materials modified with mineral admixtures such as fly ash.

4. CONCLUSIONS

This study evaluated the performance of self-compacting engineered cementitious composites (SCC-ECC) under 28-day water curing. The results confirm that optimized SCC-ECC mixtures can achieve superior fresh properties, mechanical strength, and durability, highlighting their potential as sustainable materials for structural applications in aggressive environments.

- The selected SCC-ECC mix achieved:
  1. Compressive strength exceeding 70 MPa after 28 days,
  2. Flexural strength above 14 MPa,
  3. Impact energy absorption over 17,000 J,
  4. Chloride ion penetrability is classified as very low (<750 Coulombs),
  5. Water penetration depth less than 0.5 mm, confirming its excellent impermeability.
- Scanning Electron Microscopy (SEM) analysis revealed a compact and homogeneous microstructure with strong fiber–matrix interfacial bonding and a well-formed Interfacial Transition Zone (ITZ), justifying the observed mechanical and durability performance.

- The experimental static modulus of elasticity values (18,234 to 20,010 MPa) were lower than theoretical estimates due to ECC's ductile nature but still sufficient for structural use, consistent with ECC behavior reported in literature.
- The successful use of industrial by-products such as fly ash and high-range water reducers demonstrates the environmental and economic viability of producing sustainable, durable ECC materials.
- Overall, this study confirms that proper mix optimization, particularly balancing workability and fiber dispersion, can lead to SCC-ECC with superior performance suitable for structural applications exposed to mechanical and environmental stresses.

NOMENCLATURE

Symbol	Description	Symbol	Description
E	Static modulus of elasticity, MPa	W	Hammer weight, N
f′c	Compressive cylinder strength, MPa	Sf	Flexural strength, MPa
H	Drop height in impact test, m	ε, εu, ε2	Strain (ultimate; at 40% load), %
H1, H2	L-box heights (blocking ratio = H2/H1), mm (ratio dimensionless)	μ	Poisson's ratio
N	Number of blows in impact test	εt1, εt2	Transverse strains for Poisson's ratio
P	Maximum load in flexural test, N	σ, σcr, σu	Tensile stress (first-cracking; ultimate), MPa
Q	Total charge passed in RCPT, Coulombs		

Acknowledgements

The authors gratefully acknowledge the support of the Department of Civil Engineering, University of Baghdad, for providing laboratory facilities and technical assistance throughout this study.

Credit Authorship Contribution Statement

Mohammed Shaker Amouri: Conceptualization, Methodology, Experimental work, Data curation, Formal analysis, Writing – Original draft, Visualization. Nada Mahdi Fawzi: Supervision, Resources, Validation, Review & Editing.

Declaration of Competing Interest

The authors declare that they have no known competing financial interests or personal relationships that could have appeared to influence the work reported in this paper.

REFERENCES

Abd Almajeed, S.Q., and Abbas, Z.K., 2024. Eco-friendly roller compacted concrete: a review. *Journal of Engineering*, 30(7), pp. 144–165. https://doi.org/10.31026/j.eng.2024.07.09.

Abid, S.R., Murali, G., Ahmad, J., Al-Ghasham, T.S., and Vatin, N.I., 2022. Repeated drop-weight impact testing of fibrous concrete: state-of-the-art literature review, analysis of results variation and test improvement suggestions. *Materials*, 15(11), P. 3948. https://doi.org/10.3390/ma15113948

ACI 544.2R-09, 2009. Measurement of properties of fiber reinforced concrete. American Concrete Institute, Farmington Hills, MI.

Algalawi, N.M., and Ahmad, H.I.H., 2014. Effect of local feldspar on the properties of self-compacting concrete. Journal of Engineering, 20(9), pp. 135–146. https://doi.org/10.31026/j.eng.2014.09.10.

Al-Ameri, R.A., Özakça, M., Karataş, E.E., Göğüş, M.T., and Tanrıkulu, A.H., 2022. Drop-weight impact tests on engineered cementitious composites heated to 500 °C. *Wasit Journal of Engineering Sciences*, 10(2), pp. 240–251. https://doi.org/10.31185/ejuow.vol10.iss2.409.

Al-Ameri, R.A., Abid, S.R., and Özakça, M., 2022. Mechanical and impact properties of engineered cementitious composites reinforced with PP fibers at elevated temperatures. *Fire*, 5(1), P. 3. https://doi.org/10.3390/fire5010003.

Amar, Y., Ebrahem, A.A., and Fawzi, N.M., 2017. Enhancing performance of self-compacting concrete with internal curing using thermostone chips. *Journal of Engineering*, 23(7). https://doi.org/10.31026/j.eng.2017.07.01.

Anasi, F.K., and M., S.K., 2020. Experimental investigation on engineered cementitious composite (ECC). *International Research Journal of Engineering and Technology (IRJET)*, 7(7), pp. 1803–1808.

ASTM C618-15, 2015. Standard specification for coal fly ash and raw or calcined natural pozzolan for use in concrete. ASTM International, West Conshohocken, PA. https://doi.org/10.1520/C0618-15.

ASTM C39-21, 2021. Standard test method for compressive strength of cylindrical concrete specimens. ASTM International, West Conshohocken, PA. https://doi.org/10.1520/C0039_C0039M-21.

ASTM C270-19, 2019. Standard specification for mortar for unit masonry. ASTM International, West Conshohocken, PA. https://doi.org/10.1520/C0270-19.

ACI 318-19, 2019. Building code requirements for structural concrete (ACI 318-19) and commentary. American Concrete Institute, Farmington Hills, MI. https://doi.org/10.14359/51716937.

ASTM C494/C494M-13, 2013. Standard specification for chemical admixtures for concrete. ASTM International, West Conshohocken, PA. https://doi.org/10.1520/C0494_C0494M-13.

ASTM C348-21, 2021. Standard test method for flexural strength of hydraulic-cement mortars. ASTM International, West Conshohocken, PA. https://doi.org/10.1520/C0348-21.

ASTM C469-22, 2022. Standard test method for static modulus of elasticity and Poisson's ratio of concrete in compression. ASTM International, West Conshohocken, PA.

ASTM C1202-22, 2022. Standard test method for electrical indication of concrete's ability to resist chloride ion penetration. ASTM International, West Conshohocken, PA.

Central Organization for Standardization and Quality Control (COSQC), 2018. Iraqi specification No. 1703: used water in concrete. COSQC, Baghdad, Iraq.

Choucha, S., Benyahia, A., Ghrici, M., and Mansour, M.S., 2018a. Correlation between compressive strength and other properties of engineered cementitious composites with high-volume natural pozzolana. *Asian Journal of Civil Engineering*, 19(5), pp. 639–646. https://doi.org/10.1007/s42107-018-0050-3.

COSQC (Central Organization for Standardization and Quality Control) , 2019. Iraqi Standard No. 5: Portland cement – Requirements, Baghdad, Iraq.

COSQC (Central Organization for Standardization and Quality Control) , 1984. Iraqi Standard No. 45: Aggregate from natural sources for concrete and construction, Baghdad, Iraq.

de Jesus, W.S., da Silva, S.F.M., de Almeida, T.M.S., Souza, M.T., Leal, E.S., Souza, R.S., Sacramento, L.A., Allaman, I.B., and Pessoa, J.R.C., 2025. Comparative study of ASTM C1202 and IBRACON/NT Build 492 testing methods for assessing chloride ion penetration in concretes using different types of cement. *Buildings*, 15(3), P. 302. https://doi.org/10.3390/buildings15030302.

DIN 1048-5, 1991. Testing of concrete; hardened concrete testing. DIN – Deutsches Institut für Normung, Berlin, Germany.

Ding, Y., Yu, K., and Mao, W., 2020. Compressive performance of all-grade engineered cementitious composites: experiment and theoretical model. *Construction and Building Materials*, 244, P. 118357. https://doi.org/10.1016/j.conbuildmat.2020.118357.

EFNARC, 2002. The European guidelines for self-compacting concrete: specification, production and use. EFNARC, Association House, Farnham, UK.

EN 1992-1-1, 2004. Eurocode 2: design of concrete structures – part 1-1: general rules and rules for buildings. European Committee for Standardization (CEN), Brussels, Belgium.

EN 12390-8, 2019. Testing hardened concrete – part 8: depth of penetration of water under pressure. European Committee for Standardization (CEN), Brussels, Belgium.

Ghafor, K., Ahmed, H.U., Faraj, R.H., Mohammed, A.S., Kurda, R., Qadir, W.S., Mahmood, W., and Abdalla, A.A., 2022. Computing models to predict the compressive strength of engineered cementitious composites (ECC) at various mix proportions. *Sustainability*, 14(19), P. 12876. https://doi.org/10.3390/su141912876.

Krishnaraja, A.R., and Kandasamy, S., 2018. Flexural performance of hybrid engineered cementitious composite layered reinforced concrete beams. *Periodica Polytechnica Civil Engineering*, 62(4), pp. 921–929. https://doi.org/10.3311/ppci.11748.

Lepech, M.D., and Li, V.C., 2009. Water permeability of engineered cementitious composites. *Cement and Concrete Composites*, 31(10), pp. 744–753. https://doi.org/10.1016/j.cemconcomp.2009.07.002.

Lepech, M.D. and Li, V.C., 2008. Large-scale processing of engineered cementitious composites. In: *Eco-efficient construction and building materials*. Springer, Dordrecht

Li, V.C., 2007. Engineered cementitious composites (ECC): material, structural, and durability performance. In: Nawy, E.G. (ed.), *Concrete Construction Engineering Handbook*. 2nd ed. CRC Press, Boca Raton, FL, pp. 24-1–24-38.

Li, V.C., 2012. Can concrete be bendable?: The notoriously brittle building material may yet stretch instead of breaking. *American Scientist*, 100(6), pp. 484–493. https://doi.org/10.1511/2012.100.484.

Li, V.C., and Kanda, T., 1998. Engineered cementitious composites for structural applications. In: Dhir, R.K., Henderson, N.A. and Limbachiya, M.C. (eds.), *Concrete in the Service of Mankind: Concrete for Infrastructure and Utilities*. E&FN Spon, London, pp. 213–223.

Li, V.C., and Li, V., 2005. Engineered cementitious composites. In: *Proceedings of the International Conference on Advances in Concrete and Construction Materials (CONMAT 2005)*, Hyderabad, India.

Murali, G., Santhi, A.S., and Ganesh, G.M., 2014. Impact resistance and strength reliability of fiber-reinforced concrete in bending under drop weight impact load. *International Journal of Technology*, 5(2), pp. 111–120. https://doi.org/10.14716/ijtech.v5i2.403.

Naderi, M., Kaboudan, A., and Sadighi, A.A., 2018. Comparative Study on Water Permeability of Concrete Using Cylindrical Chamber Method and British Standard and Its Relation with Compressive Strength ARTICLE INFO ABSTRACT. *Journal of Rehabilitation in Civil Engineering*, [online] 6(1), pp. 116–131. https://doi.org/10.22075/JRCE.2018.13489.1247.

Nalon, G.H., Martins, R.O.G., Alvarenga, R.C.S.S., Lima, G.E.S., Pedroti, L.G., and Santos, W.J., 2017. Effect of specimens' shape and size on the determination of compressive strength and deformability of cement-lime mortars. *Materials Research*, 20(4), pp. 819–825. https://doi.org/10.1590/1980-5373-mr-2016-1006.

Qorllari, A., and Bier, T.A., 2022. Optimization of workability and compressive strength of self-compacting mortar using screening design. *CivilEng*, 3(4), pp. 998–1012. https://doi.org/10.3390/civileng3040056.

Pontes, J., Bogas, J.A., Real, S., and Silva, A., 2021. The Rapid Chloride Migration Test in Assessing the Chloride Penetration Resistance of Normal and Lightweight Concrete. *Applied Sciences*, 11(16), P. 7251. https://doi.org/10.3390/app11167251

Raharjo, D., Subakti, A., and Tavio, 2013. Mixed concrete optimization using fly ash, silica fume and iron slag on the SCC's compressive strength. *Procedia Engineering*, 54, pp. 827–839. https://doi.org/10.1016/j.proeng.2013.03.076.

Safarkhani, M., and Naderi, M., 2023. Enhanced impermeability of cementitious composite by different content of graphene oxide nanoparticles. *Journal of Building Engineering*, 72, P. 106675. https://doi.org/10.1016/j.jobe.2023.106675.

Şahmaran, M., and Li, V.C., 2009. Influence of microcracking on water absorption and sorptivity of ECC. Materials and Structures, 42(5), pp. 593–603. https://doi.org/10.1617/s11527-008-9406-6.

Salah, S., Fawzi, N.M., and Ahmed, I.F., 2021. Time Dependent Behavior of Engineered Cementitious Composite Concrete Produced from Portland Limestone Cement. In: *IOP Conference Series: Earth and Environmental Science*. IOP Publishing Ltd. https://doi.org/10.1088/1755-1315/856/1/012016.

Salih, A.A., and Ahmed, I.F., 2013. Combined effect of fineness modulus and grading zones of fine aggregate on fresh properties and compressive strength of self-compacted concrete. Journal of Engineering, 19(6), pp. 774–785. https://doi.org/10.31026/j.eng.2013.06.09

Shen, Y., Li, Q., Huang, B., Liu, X., and Xu, S., 2022. Effects of PVA fibers on microstructures and hydration products of cementitious composites with and without fly ash. *Construction and Building Materials*, 360, P. 129533. https://doi.org/10.1016/j.conbuildmat.2022.129533.

Shi, C., 2004. Effect of mixing proportions of concrete on its electrical conductivity and the rapid chloride permeability test (ASTM C1202 or AASHTO T277) results. *Cement and Concrete Research*, 34(3), pp. 537–545. https://doi.org/10.1016/j.cemconres.2003.09.007.

Sika Iraq (Sika Trading L.L.C.). Sika® ViscoCrete®-180 GS – Product Data Sheet. Version 04.01, December 2022.

Skutnik, Z., Sobolewski, M., and Koda, E., 2020. An experimental assessment of the water permeability of concrete with a superplasticizer and admixtures. *Materials*, 13(24), pp. 1–16. https://doi.org/10.3390/ma13245624.

Turk, K., Kina, C., and Nehdi, M.L., 2022. Durability of Engineered Cementitious Composites Incorporating High-Volume Fly Ash and Limestone Powder. *Sustainability*, 14(16). https://doi.org/10.3390/su141610388.

Wang, Q., Qi, Y., Yi, Y., and He, P., 2023. Characterizing interfacial properties of PVA fiber reinforced cementitious composites with different mechanical properties. *SSRN Electronic Journal*. https://ssrn.com/abstract=4501186.

Wu, H., Yu, J., Zhou, J., Li, W., and Leung, C.K.Y., 2021. Experimental study on chloride-induced corrosion of soil nail with engineered cementitious composites (Ecc) grout. *Infrastructures*, 6(11). https://doi.org/10.3390/infrastructures6110161.

Xiong, Y., Yang, Y., Fang, S., Wu, D., and Tang, Y., 2021. Experimental research on compressive and shrinkage properties of ECC containing ceramic wastes under different curing conditions. *Frontiers in Materials*, 8, P. 727273. https://doi.org/10.3389/fmats.2021.727273.

Yaseen, N., Sahar, U., Bahrami, A., Saleem, M.M., Iqbal, M.A., and Siddique, I., 2023. Synergistic impacts of fly ash and sugarcane bagasse ash on performance of polyvinyl alcohol fiber-reinforced engineered cementitious composites. *Results in Materials*, 20, P. 100490. https://doi.org/10.1016/j.rinma.2023.100490.

Zhang, P., Li, Q.F., Wang, J., Shi, Y., and Ling, Y.F., 2019. Effect of PVA fiber on durability of cementitious composite containing nano-SiO_2. *Nanotechnology Reviews*, 8(1), pp. 116–127. https://doi.org/10.1515/ntrev-2019-0011.

Zhang, P., Sun, X., Wei, J., Wang, J., and Gao, Z., 2023a. Influence of PVA fibers on the durability of cementitious composites under the wet-heat-salt coupling environment. *Reviews on Advanced Materials Science*, 62(1), P. 20230155. https://doi.org/10.1515/rams-2023-0155.

Zhang, S., He, S., Ghiassi, B., van Breugel, K., and Ye, G., 2023b. Interface bonding properties of polyvinyl alcohol (PVA) fiber in alkali-activated slag/fly ash. *Cement and Concrete Research*, 173, P. 107308. https://doi.org/10.1016/j.cemconres.2023.107308.

تقييم أداء الخرسانة الأسمنتية المهندسة ذاتية الدمك (SCC-ECC) تحت ظروف المعالجة العادية لمدة 28 يومًا

محمد شاكر اموري*، ندى مهدي فوزي

قسم الهندسة المدنية، كلية الهندسة، جامعة بغداد، بغداد، العراق

الخلاصة

تهدف هذه الدراسة إلى تقييم أداء الخرسانة الأسمنتية المركبة ذاتية الدمك (SCC-ECC) تحت ظروف المعالجة المائية القياسية لمدة 28 يومًا، بهدف تطوير خلطة تمتاز بقابلية انسياب مثلى، وقوة ميكانيكية عالية، ومتانة محسّنة. جرى تحضير سبعٍ وعشرين خلطة من مونة SCC-ECC (بدون ركام خشن) واختبارها وفق متطلبات EFNARC (2002) الخاصة بالمونة ذاتية الدمك. وأظهرت نتائج الفحوصات الطازجة (هطول الانسياب 240–260 مم، زمن قمع V بين 6–12 ثانية، ونسبة صندوق L أكبر من 0.80) أن الخلطات تحقق قابلية انسياب جيدة. بالإضافة إلى ذلك، أثبتت اختبارات الشد المباشر على نماذج الـ dog-bone سلوك التصلب بالشد (strain-hardening) مع ظهور تشققات دقيقة متعددة وسعة انفعال تجاوزت 2%، مما يؤكد أن المادة تتمتع بخصائص ECC. وقد تم تحضير الخلطات باستخدام نسب مختلفة من الرماد المتطاير (20%، 25%، 30%)، وألياف البولي فينيل الكحول (1.5%–2.0%)، ومضافات تقليل الماء عالية الكفاءة. وجرى تحديد الخلطة المثلى (R2) بناءً على تفوقها في مقاومة الانضغاط، مقاومة الانحناء، مقاومة الصدمات، نفاذية الماء، ومعامل المرونة. إذ حققت هذه الخلطة مقاومة انضغاط تجاوزت 70 ميغاباسكال، ومقاومة انحناء فاقت 14 ميغاباسكال، وامتصاص طاقة صدمية يزيد على 17,000 جول، مع نفاذية منخفضة جدًا للكلوريدات (<750 كولومب). كما أكّد الفحص بالمجهر الإلكتروني الماسح (SEM) أن البنية المجهرية كثيفة مع تماسك قوي بين الألياف والمصفوفة. وتبرهن النتائج على إمكانية إنتاج SCC-ECC يتمتع بخصائص ممتازة في حالتيه الطرية والمتصلبة، باستخدام منتجات صناعية ثانوية ومضافات محسّنة للأداء، بما يدعم تطوير مواد إنشائية مستدامة وذات أداء عالٍ مناسبة للتطبيقات في البيئات القاسية.

الكلمات المفتاحية: الخرسانة الأسمنتية المهندسة، ذاتية الرص، ألياف PVA، الرماد المتطاير، معالجة عادية